**Molecular Human Reproduction, Vol.26, No.4, pp. 215–227, 2020**
Advance Access Publication on February 3, 2020 doi:10.1093/molehr/gaaa011

molecular human reproduction

ORIGINAL RESEARCH

# Differential tissue-specific damage caused by bacterial epididymo-orchitis in the mouse

**Britta Klein [1,*], Sudhanshu Bhushan [1], Stefan Günther [2], Ralf Middendorff [1], Kate L. Loveland [3,4], Mark P. Hedger [3,4], and Andreas Meinhardt [1,3,*]**

[1]Institute of Anatomy and Cell Biology, Justus-Liebig University of Giessen, Giessen 35385, Germany [2]ECCPS Bioinformatics and Deep Sequencing Platform, Max Planck Institute for Heart and Lung Research, Bad Nauheim 61231, Germany [3]Centre for Reproductive Health, Hudson Institute of Medical Research, Clayton 3168, Australia [4]Department of Molecular and Translational Sciences, School of Clinical Sciences, Monash University, Monash Medical Centre, Clayton 3168, Australia

*Correspondence address. Institute of Anatomy and Cell Biology, Justus-Liebig University of Giessen, Aulweg 123, 35398 Giessen, Germany. Fax: +49-641-994168; E-mail: britta.klein@anatomie.med.uni-giessen.de https://orcid.org/0000-0001-7892-069X Institute of Anatomy and Cell Biology, Justus-Liebig University of Giessen, Aulweg 123, 35398 Giessen, Germany. Fax: +49-641-9947024; E-mail: andreas.meinhardt@anatomie.med.uni-giessen.de https://orcid.org/0000-0003-3711-2746

*Submitted on July 30, 2019; resubmitted on January 13, 2020; editorial decision on January 24, 2020*

**ABSTRACT:** Ascending bacterial urinary tract infections can cause epididymo-orchitis. In the cauda epididymidis, this frequently leads to persistent tissue damage. Less coherent data is available concerning the functional consequences of epididymo-orchitis on testis and caput epididymidis. This *in vivo* study addresses the functional and spatial differences in responsiveness of murine epididymis and testis to infection with uropathogenic *Escherichia coli* (UPEC). Whole transcriptome analysis (WTA) was performed on testis, caput, corpus and cauda epididymidis of adult C57BL/6 J wildtype mice. Following UPEC-induced epididymo-orchitis in these mice, epididymal and testicular tissue damage was evaluated histologically and semi-quantitatively at 10 days and 31 days post-inoculation. Expression of inflammatory markers and candidate antimicrobial genes were analysed by RT-qPCR. WTA revealed distinct differences in gene signatures between caput and cauda epididymidis, particularly amonst immunity-related genes. Cellular and molecular signs of testicular inflammation and disruption of spermatogenesis were noticed at day 10, but recovery was observed by day 31. In contrast to the cauda, the caput epididymidis did not reveal any signs of gross morphological damage or presence of pro-inflammatory processes despite confirmed infection. In contrast to beta-defensins, known UPEC-associated antimicrobial peptides (AMP), like *Lcn2, Camp* and *Lypd8*, were inherently highly expressed or upregulated in the caput following infection, potentially allowing an early luminal protection from UPEC. At the time points investigated, the caput epididymidis was protected from any obvious infection/inflammation-derived tissue damage. Studies addressing earlier time-points will conclude whether in the caput epididymidis a pro-inflammatory response is indeed not essential for effective protection from UPEC.

**Key words:** uropathogenic *E. coli* / testis / epididymis / epididymo-orchitis / spermatogenesis / beta-defensin / LYPD8

## Introduction

Acute epididymo-orchitis (AEO) is the most common cause of intrascrotal inflammation and accounts for 600 000 medical visits per year in the USA alone (Banyra & Shulyak, 2012; Street *et al.*, 2017). The most common pathogen isolated from acute epididymo-orchitis (AEO) in the clinic are *E. coli* pathovars such as uropathogenic *E. coli* (UPEC). Bacterial AEO is commonly preceded by an acute epididymitis that, in 60% of patients, subsequently spreads to the testis (Schuppe *et al.*, 2010) and regularly results in sub- or infertility even following antimicrobial treatment (Pilatz *et al.*, 2016). Fertility impairment following AEO can originate from permanent epididymal damage with ductal obstructions aggravating or hindering sperm transit, whereas direct exposure of testicular germ cells to bacterial pathogens, pathogen-derived toxins or subsequently derived immune factors can also cause damage to spermatogenesis itself (Schuppe *et al.*, 2008; Schuppe *et al.*, 2010; Bhushan *et al.*, 2011; Pilatz *et al.*, 2013).

Consistently, the cauda epididymidis has been identified in a number of studies to be particularly sensitive to bacterial AEO and concomitant inflammation resulting in long-term damage (Pilatz *et al.*, 2013; Michel *et al.*, 2015; Michel *et al.*, 2016; Fijak *et al.*, 2018; Klein *et al.*, 2019). Studies on the testicular consequences of AEO are more rare, especially in humans. For example, an increase in testicular volume (usually due to oedema formation), concomitant with a

decrease of sperm numbers and other ejaculate parameters, has been reported (Pilatz et al., 2013). In long-term follow-up studies, persistent oligo(asthenoterato)zoospermia was diagnosed in ~30% of cases with a further 10% suffering from azoospermia (Schuppe et al., 2010; Rusz et al., 2012; Schuppe et al., 2017). Complete testicular recovery after an incidence of AEO was reported in one further study (Pilatz et al., 2013).

Surprisingly, the caput epididymidis appears to remain essentially unaffected during bacterial AEO, despite confirmed bacterial transit in rodents (Biswas et al., 2015; Michel et al., 2016; Fijak et al., 2018). This may be due to a reduced capacity for inflammatory or immune responses, likely manifested by a tissue-specific gene expression signature (Michel et al., 2015) as exemplified by the highly differential expression of epididymal beta-defensins as antimicrobial peptides in caput versus cauda epididymidis (Ribeiro et al., 2012). It needs to be noted, however, that the antimicrobial function and importance of epididymal beta-defensins to combat infections is not well understood. Considerations are further complicated by opposing observations: on the one hand, beta-defensin-overexpressing mice showed resistance to bacterial invasion of the epididymis and an induction of beta-defensins during bacterial AEO was noted, whereas on the other hand a decrease in epididymal beta-defensin levels was documented following an inflammatory challenge with bacterial lipopolysaccharide (LPS) (Cao et al., 2010; Fei et al., 2012; Biswas et al., 2015).

This study aimed to elucidate the differential immune responsiveness of testis and caput versus cauda epididymidis to bacterial infection using whole transcriptome analysis and an established mouse model of UPEC-induced AEO to assess differences in tissue reactivity with special focus on the short- and long-term effects of AEO on testis and caput epididymidis.

# Materials and Methods

## Ethics statement

Animal experiments were approved by the responsible committee on animal care (Regierungspraesidium Giessen GI 20/25 Nr. G 60/2017) and carried out in strict accordance with the recommendations of the Guide for the Care and Use of Laboratory Animals of the German law of animal welfare.

## Induction of bacterial AEO in mice, treatment groups

Uropathogenic *E. coli* (UPEC) strain CFT073 was cultured as described previously (Michel et al., 2016). Adult C57BL/6J male mice (Charles River Laboratories, Sulzfeld, Germany; 10–12 weeks of age) were anesthetised with an intraperitoneal injection of ketamine and xylazine, and bacterial AEO was induced by injection of UPEC via the vas deferens, as described previously (Klein et al., 2019). Sham-treated controls were injected with phosphate-buffered saline instead of UPEC. Mice were killed at Day 10 and Day 31 post-inoculation (p.i.), and testes and epididymides were snap-frozen for subsequent RNA analysis, fixed for histological examination or homogenised for determination of bacterial colony-forming units (CFU). Time points were chosen based on the following data acquired by Michel et al. (2016). At Day 3 p.i., bacteria were present in the cauda epididymidis, but barely any histological damage was apparent. At Day 7 p.i., bacteria had ascended to the testis with severe damage evident in the cauda epididymidis. Thus, damage in the cauda was suggested to develop between Day 3 and Day 7 p.i. With bacteria ascending to the testis past the caput by Day 7 p.i., an assessment at Day 10 p.i. would allow sufficient time for any possible pathological alteration to become visible in the caput epididymidis. Day 31 p.i. was chosen to analyse a possible progressive 'silent' deterioration or improvement after a sufficiently longer period of time.

## Histological and immunohistochemical analysis

Sections of Bouin's fixed (4 h) tissues were stained with haematoxylin and eosin (testis) or Sirius Red (epididymis). An adaptation of the classical Johnsen scoring system (Johnsen, 1970) of spermatogenesis was used, whereby the overall presence or absence of certain germ cell types in each tubule cross-section was assessed, rather than their quantitative abundance. In more detail, spermatogenic disturbance was assessed by evaluating 200 seminiferous tubule cross-sections per mouse and recording the most advanced germ cell type detectable in each tubule cross-section and finally documenting the percentage of tubule cross-sections showing the respective germ cell stage. Hence criterium ES (elongated spermatids) is related to Johnsen scores 10-8; RS (round spermatids) is related to Johnsen scores 7-6; PSc (pachytene spermatocytes) is related to Johnsen scores 5-4; SG (spermatogonia) is related to Johnsen score 3; SCO (Sertoli-cell only) is related to Johnsen score 2; Johnsen score 1 (complete absence of seminiferous epithelium) was not observed. For the detection of proliferating cells, sections of Bouin's fixed testes were stained with an anti-PCNA antibody (1:500 dilution, product no. ab92552, Abcam, Cambridge, UK). For each testis, 200 seminiferous tubule cross-sections were examined for PCNA-positive germ cells. For the detection of F4/80-positive mononuclear phagocytes, testicular acetone-fixed cryosections were stained with an anti-F4/80 antibody (1200 dilution, product no. MCA497G, Bio-Rad, Munich, Germany). The respective numbers of mice studied were as follows: sham-treated 10 days, $n = 3$; UPEC 10 days, $n = 4$; sham-treated 31 days, $n = 3$; UPEC 31 days, $n = 4$.

## Determination of CFU

Testis, caput and cauda epididymidis samples from sham-treated and UPEC-infected mice at 10 days p.i. were homogenised in sterile PBS ($n = 2$ per group). Ten-fold serial dilutions of tissue homogenates were prepared, and 100 µl of each dilution was streaked onto LB (lysogeny broth) agar plates. After 24 h at 37°C, CFU were counted and the respective CFU/ml was calculated.

## Quantitative real-time RT-PCR

Total RNA was isolated from testis, caput and cauda epididymidis of wild-type, sham-treated and UPEC-infected mice using TRIzol™ reagent (Thermo Fisher Scientific, MA, USA) and RNeasy Mini Kit (Qiagen, Hilden, Germany), including on-column DNase digestion. Real-time RT-qPCR was performed using iTaq Universal SYBR Green Supermix (Bio-Rad, Munich, Germany) and the CFX Touch™ Real-Time PCR detection system (Bio-Rad). Details of the primer pairs

used are summarised in Supplementary Table SI. DNA was isolated and used in qPCR for detection of the bacterial marker gene *PapC* as an indicator for the tissue-inherent bacterial load (see Lu *et al*., 2013; Biswas *et al*., 2015; Michel *et al*., 2016; Klein *et al*., 2019). All target gene expression measurements were normalised to a stable housekeeping gene, *Rplp0* (60S ribosomal protein, large, P0). The mRNA expression levels are presented as relative fold changes normalised to the sham-treated control samples, calculated by the $2^{(-ddCT)}$ method or as relative expression, calculated by $2^{(-dCT)}$, respectively. The respective numbers of mice studied were as follows: sham 10 days, testis $n = 6$, caput $n = 4$, cauda $n = 4$; UPEC 10 days, testis $n = 5$, caput $n = 4$, cauda $n = 6$; wild-type, testis $n = 3$, caput $n = 3$, cauda $n = 3$.

## WTA and gene expression analysis

Total RNA was isolated from testis, caput, corpus and cauda epididymidis of three male C57BL/6J wild-type mice as described above. Total RNA and library integrity were verified with LabChip Gx Touch 24 (Perkin Elmer, MA, USA), and 1 µg of total RNA was used as input for SMARTer Stranded Total RNA Sample Prep Kit—HI Mammalian (Clontech, CA, USA) following the manufacturer's protocol. Sequencing was performed on the NextSeq 500 instrument (Illumina, CA, USA) using v2 chemistry, resulting in average of 49M reads per library with 1x75bp single end setup. The resulting raw reads were assessed for quality, adapter content and duplication rates with FastQC (Andrews, 2010). Trimmomatic version 0.33 was employed to trim reads after a quality drop below a mean of Q20 in a window of five nucleotides (Bolger *et al*., 2014). Only reads between 30 and 150 nucleotides were cleared for further analyses. Trimmed and filtered reads were aligned versus the Ensembl mouse genome version mm10 (GRCm38) using STAR 2.4.0a with the parameter '–outFilterMismatchNoverLmax 0.1' to increase the maximum ratio of mismatches to mapped length to 10% (Dobin *et al*., 2013). The number of reads aligning to genes was counted with featureCounts 1.4.5-p1 tool from the Subread package (Liao *et al*., 2013). Only reads mapping at least partially inside exons were admitted and aggregated per gene. Reads overlapping multiple genes or aligning to multiple regions were excluded. Differentially expressed genes were identified using DESeq2 version 1.62 (Love *et al*., 2014). Only genes with a minimum fold change of $+-1.5$ ($\log2+-0.59$), a maximum Benjamini–Hochberg corrected *P* value of 0.05, and a minimum combined mean of five reads were deemed to be significantly differentially expressed. The Ensemble annotation was enriched with UniProt data (release 06.06.2014) based on Ensembl gene identifiers (UniProt Consortium, 2014). Data are deposited at GEO (https://www.ncbi.nlm.nih.gov/geo/query/acc.cgi?acc=GSE141071). Data in graphs is presented as *Z*-score. This normalisation method can meaningfully compare widely different distributions. It is defined as the number of standard deviations that a value is above or below the mean of all values. Data in Supplementary Table SII are presented as library-size normalised counts.

## Lypd8 assessment and functional *in vitro* analysis

Laser-assisted microdissection (PALM CombiSystem, Zeiss, Wetzlar, Germany) was performed on 7-µm-thick sections of Bouin's-fixed paraffin-embedded wild-type epididymis. Caput epithelium and caput interstitium were selectively excised and introduced to RNA-processing and RT-qPCR analysis of *Lypd8* expression as described above. MEPC5 cells (mouse caput epididymal epithelial cell line) (Tabuchi *et al*., 2005) were cultured in DMEM/F12 (1,1) (Gibco, Waltham, MA, USA), supplemented with 10% foetal bovine serum (Gibco) and 1% penicillin/streptomycin (Gibco), at 33°C with 5% $CO_2$. Cells were grown in six-well plates at ~90% confluency and challenged with UPEC CFT073 (multiplicity of infection (MOI) three bacteria:cells). To assess the effects of LYPD8 on bacterial adherence to epididymal epithelial cells *in vitro*, UPEC were pre-incubated for 1 h on ice with or without 1 µg/ml human recombinant LYPD8 (product no. 9087-C4, Novus Biological, CO, USA) (Okumura *et al*., 2016) before infection of MEPC5 cells. A standard bacterial adherence assay was then performed as described by Letourneau *et al*. (2011). In detail, culture supernatants and PBS washes containing non-adherent bacteria as well as MEPC5 cells with adherent bacteria were collected separately, serially diluted and plated onto LB agar plates. CFU were determined after incubation of agar plates at 37°C for 24 h. For statistical analysis, an unpaired *t* test was performed, comparing CFU in MEPC5 fractions challenged with UPEC that were pre-incubated with or without recombinant LYPD8. MOI 3 (bacteria:cells) was chosen because higher MOI or incubation times induced rapid epithelial cell detachment and damage (Welch, 2016; Terlizzi *et al*., 2017). A short-term 4°C co-culture of UPEC CFT073 and MEPC5 cells was chosen as standard co-culture condition to prevent any UPEC proliferation that would otherwise potentially mask any LYPD8 effect by increasing the proportion of LYPD8-unaffected UPEC.

## Statistical analysis

Data are expressed as mean ± SD or as box-and-whisker plots with median, first and third quartile and minimum/maximum values. Statistical analyses were performed using IBM SPSS Statistics for Windows, Version 22.0, released 2013 (IBM Corporate, NY, USA) and GraphPad Prism 6 software (GraphPad Software, CA, USA). In all cases, data were tested for normal distribution and homogeneity of variance. Based on those results, a parametric test (unpaired *t* test, significance indicated with *) or non-parametric test (Mann–Whitney *U* test, significance indicated with #) was performed for each organ, comparing sham to UPEC-infected mice. *P* values $< 0.05$ were considered to represent statistically significant differences.

# Results

## Histopathology of testis and caput epididymidis

Normal testis histology with complete spermatogenesis was observed in sham-treated control mice at 10 and 31 days p.i. (Fig. 1A and D). Bacteria were not detected in tissues of sham controls at the time points investigated (Supplementary Fig. S1A). In UPEC-infected mice at 10 days p.i., the seminiferous epithelium showed impaired spermatogenesis with vacuolisation of the germinal epithelium, presence of multinucleated cells and loss of germ cells with some tubules containing Sertoli cells only (Fig. 1B). In the interstitial space, cellular infiltrates were obvious at Day 10 p.i. (Fig. 1B), but not at Day 31 p.i. when overall testicular histology appeared similar to sham controls (Fig. 1D and E). Analysis of CFU and the bacterial gene PapC confirmed the spread of

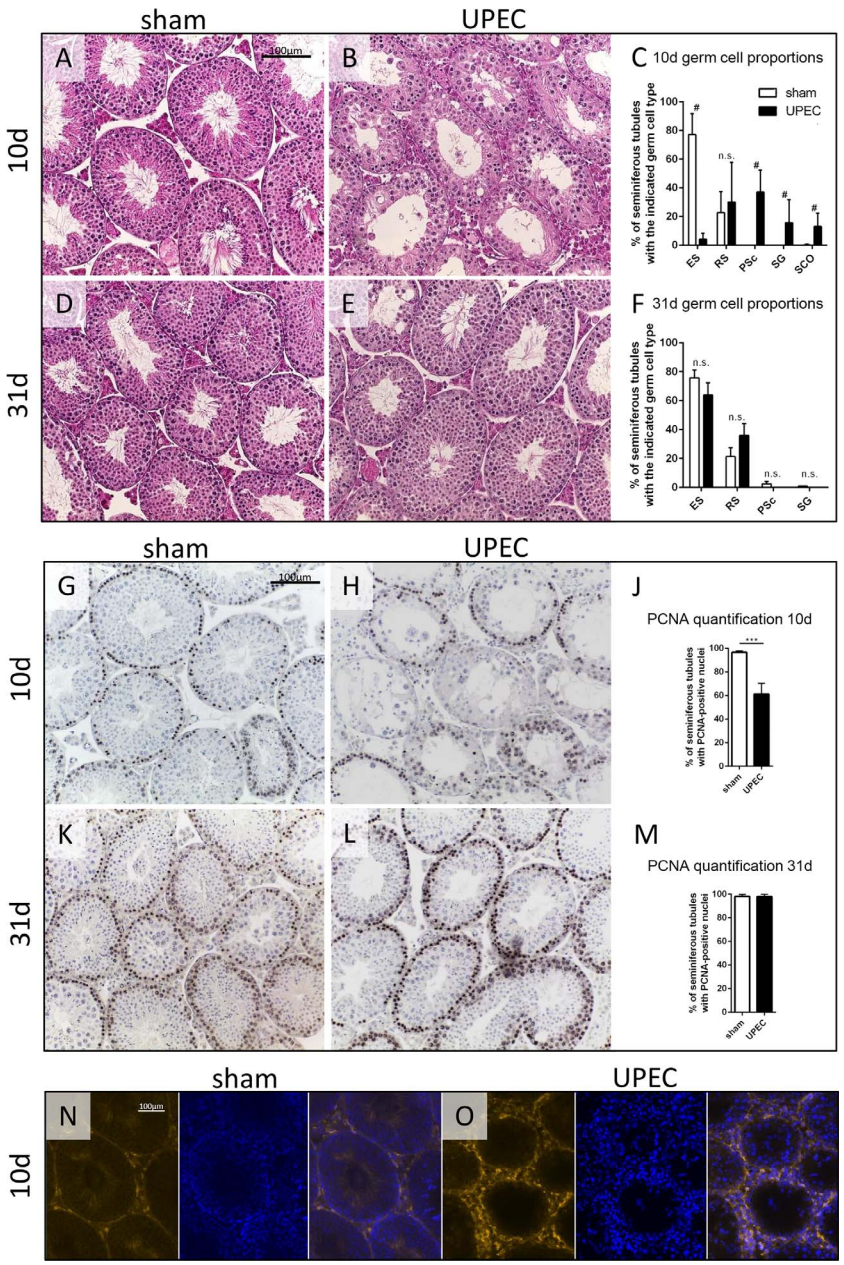


**Figure 1 Histopathological analysis of testis in UPEC-elicited mouse epididymo-orchitis.** Representative micrographs of (**A**,**B**,**D**,**E**) HE-stained and (**G**,**H**,**K**,**L**) PCNA-stained testicular sections from sham-treated controls and UPEC-infected mice 10 and 31 days after infection, respectively. (B) Sham (10 days 1A,G; 31 days 1D,K), UPEC (10 days 1B,H, 31 days 1E,L). Scale bar in panel A applies to 1A–L. (**C**,**F**) An adaptation of the classical Johnsen scoring system (Johnsen, 1970) was applied: 200 seminiferous tubule cross-sections per animal were examined and the most advanced germ cell type per tubule documented. Results are presented as the percentage of seminiferous tubule cross-sections containing the indicated germ cell type as the most advanced stage. Analyses were performed on tissue sections of sham and UPEC mice, 10 days (C) and 31 days (F) after infection, respectively. ES = elongated spermatids, RS = round spermatids, PSc = pachytene spermatocytes, SG = spermatogonia, SCO = Sertoli-cell-only. (**J**,**M**) Quantification of testicular PCNA-positive cells in sham and UPEC-infected mice 10 days (J) and 31 days (M) after infection. Two hundred tubule cross-sections were assessed for the presence (+) or absence (−) of PCNA-positive cells. Results are demonstrated as the percentage of seminiferous tubule cross-sections containing or not containing PCNA-positive cells. (N,0) Representative immunofluorescence image of 8-µm-thick acetone-fixed testicular cryosections from sham (N) and UPEC-infected mice (0) 10 days after infection, stained with an anti-F4/80 antibody (1200 dilution, product no. MCA497G, Bio-Rad, Munich, Germany), counterstained with DAPI. (C,F) Mann–Whitney *U* test for each category, comparing sham to UPEC-infected mice (####$P < 0.0001$, ###$P < 0.001$, ##$P < 0.01$, #$P < 0.05$). (J,M) Unpaired *t* test for each time-point, comparing sham to UPEC-infected mice (****$P < 0.0001$, ***$P < 0.001$, **$P < 0.01$, *$P < 0.05$). Sham 10 days, $n = 3$; UPEC 10 days, $n = 4$; sham 31 days, $n = 3$, UPEC 31 days, $n = 4$.

UPEC from the injection site (vas deferens) to the testis by Day 10 p.i. (Supplementary Fig. S1A and B).

Using an adapted Johnsen scoring system for assessing the spermatogenic damage/status, full spermatogenesis including the presence of elongated spermatids (ES) was seen in sham controls in ~80% of tubule cross-sections at Day 10 and Day 31 p.i. (Fig. 1C and F). In contrast, ES were barely detectable in UPEC-infected mice at 10 days p.i., whilst RS or meiotic pachytene spermatocytes (PSc) were found as the most advanced germ cell types in the majority of tubule cross-sections with some inter-individual differences (Fig. 1C). Tubules containing spermatogonia (SG) as the only germ cell type as well as tubules containing Sertoli-cells only (SCO) were also evident at a lower percentage (Fig. 1C). At Day 31 p.i., spermatogenesis had recovered in UPEC-infected mice, as revealed by similar germ cell proportions compared with sham control mice (Fig. 1F). Of note, despite a significant reduction compared to sham control mice, PCNA-positive spermatogonia and pachytene spermatocytes were still detectable in ~60% of tubule cross-sections in testes of UPEC-infected mice 10 days p.i. (Fig. 1G–J). This indicates that despite the damage, spermatogenic capacity was not completely eradicated in infected testes, leaving potential for recovery (Fig. 1G–J). At Day 31 p.i., PCNA-staining of testis sections from UPEC-infected mice showed no obvious differences to those from sham controls (Fig. 1K–M). Additionally, an increase in the population of interstitial F4/80-positive mononuclear phagocytes was observed in testicular cryosections of UPEC-infected mice 10 days p.i. (Fig. 1O), as opposed to sham controls (Fig. 1N). No intratubular F4/80-positive cells were observed in the testes of UPEC-infected mice.

Histological analysis of epididymal sections revealed no evident differences in the caput epididymidis of UPEC-infected mice compared with sham controls both at 10 and 31 days p.i., even though viable *E. coli* were present (Fig. 2A–H, Supplementary Fig. S1A and B). In more detail, neither changes to the cellular composition of the caput interstitium (e.g. by immune cell infiltration or collagen deposition) nor changes to the caput epithelium (e.g. by desquamation of epithelial cells, cell loss or damage) were appreciable. In contrast, persistent tissue damage was observed in the cauda epididymidis of UPEC-infected mice at both time points (Supplementary Fig. S2A–D) as reported previously (Klein *et al.*, 2019). Overall, as an indication for the number of viable UPEC, CFU were highest in the cauda, with much lower numbers found in the testis and caput epididymidis (Supplementary Fig. S1A).

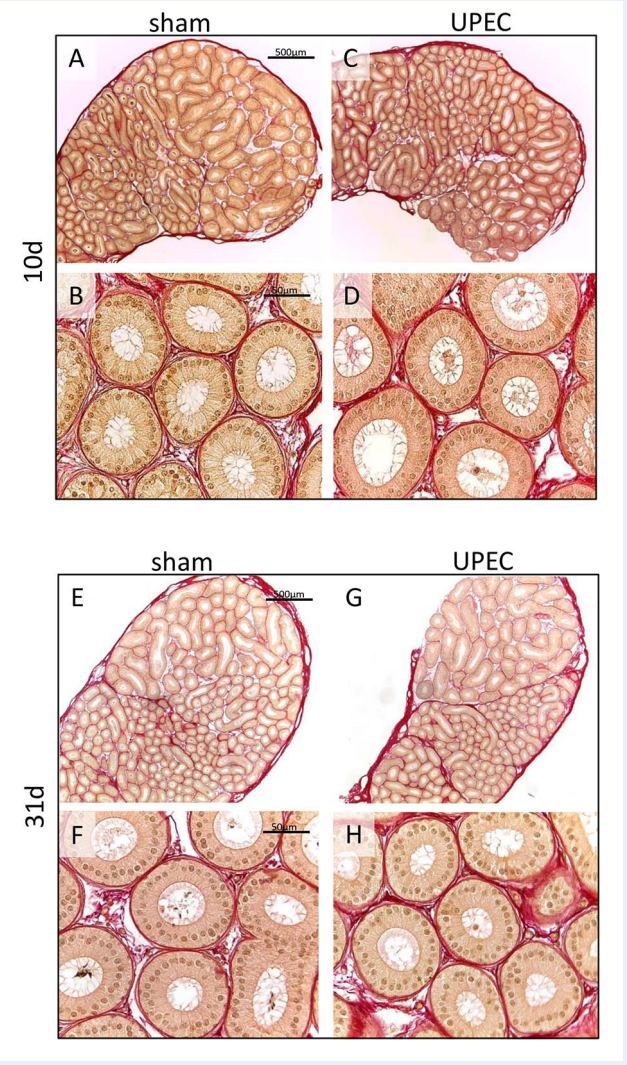


**Figure 2 Histopathological analysis of caput epididymidis in UPEC-elicited mouse epididymo-orchitis.** Representative micrographs of Sirius Red-stained epididymis sections from sham-treated controls and UPEC-infected mice 10 and 31 days after infection, respectively. Sham (10 days 2**A**,**B**, 31 days 2**E**,**F**), UPEC (10 days 2**C**,**D**, 31 days 2**G**,**H**). Scale bar in panel A applies to A,C,E,G; scale bar in panel B applies to B,D,F,H. Sham 10 days, $n = 3$; UPEC 10 days, $n = 4$; sham 31 days, $n = 3$, UPEC 31 days, $n = 4$.

## Expression analysis of immune response-associated genes in testis and caput epididymidis

RT-qPCR analysis revealed that, in samples obtained from testis and caput epididymidis of UPEC-infected mice 10 days p.i., expression levels of *Il6* (immuno-regulatory), *Il10* (anti-inflammatory) and *Tnf* (pro-inflammatory) were not significantly changed compared to sham controls (Fig. 3A). *Cxcl2*, *Nlrp3* and *Cox2* mRNA levels were analysed to help determine a possible involvement of the NLRP3-inflammasome following UPEC-infection (Fig. 3B). In this regard, *Cxcl2* was found to be non-significantly increased in UPEC-infected mice in both testis and caput epididymidis. In testis samples, a significant increase in *Nlrp3* mRNA was observed along with a significant increase of the downstream marker *Cox2* (Fig. 3B). In contrast, *Nlrp3* mRNA expression was significantly reduced in caput epididymidis samples, whilst *Cox2* mRNA expression was not significantly different to sham controls (Fig. 3B). The macrophage chemoattractant, *Ccl2*, and F4/80, a general macrophage marker, were both significantly increased in testes of UPEC-infected mice 10 days p.i., with no significant changes detectable in the caput epididymidis (Fig. 3C). Notably, changes in the samples' cellular composition/cell proportions induced by the UPEC infection (here most evident for the testis) could skew mRNA levels, allowing no definite final interpretation.

## WTA, differential expression of immunity-related genes

RNA-seq WTA of testis and caput, corpus and cauda epididymidis from three adult C57BL/6J wild-type mice was performed. Generally,

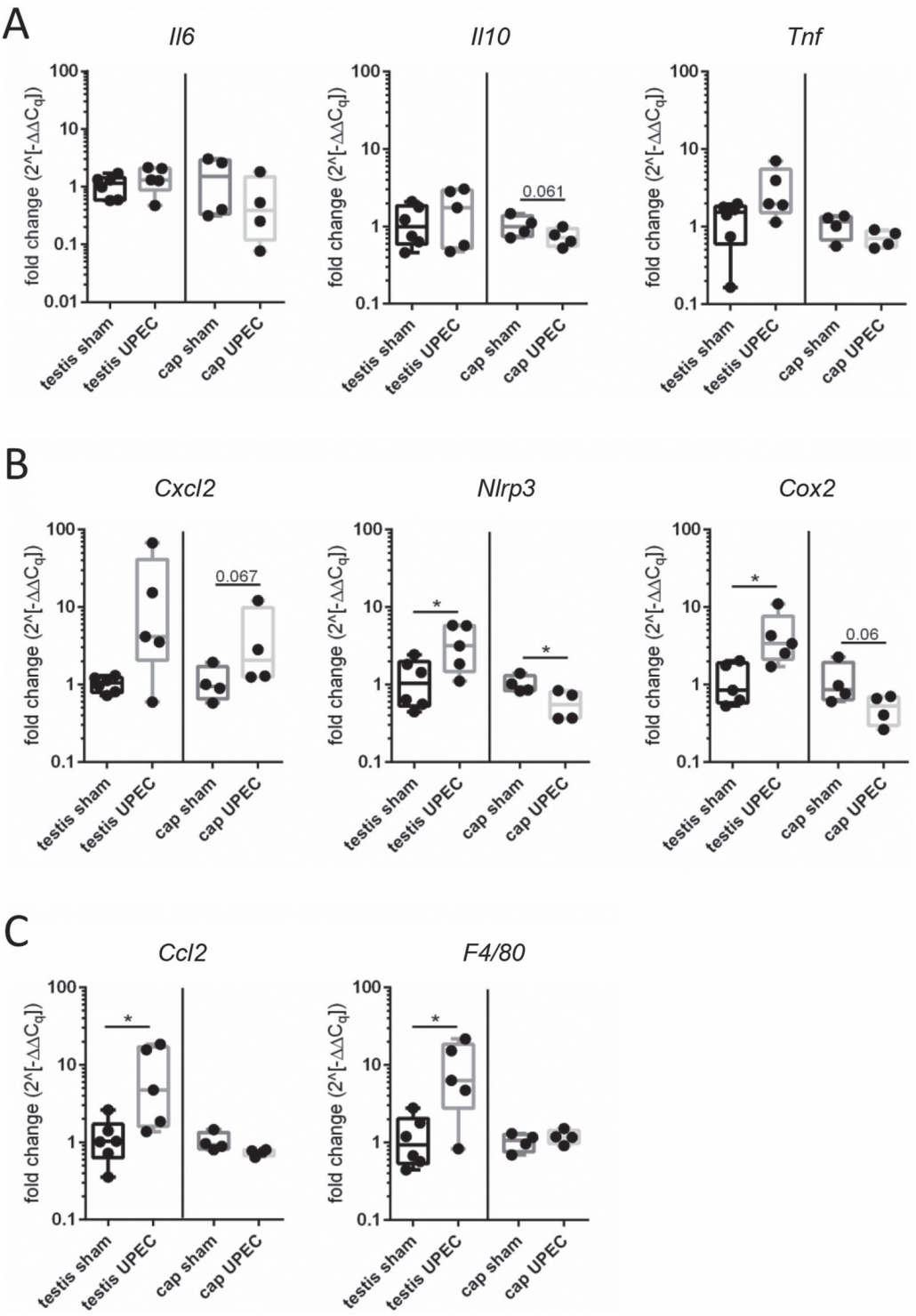


**Figure 3 RT-qPCR analysis and comparison of cytokine response in testis and caput epididymidis of sham and UPEC-infected mice 10 days after infection.** (**A**) Classical inflammatory markers, (**B**) inflammasome-associated markers, (**C**) macrophage-associated markers. Unpaired *t* test for each organ, comparing sham to UPEC-infected mice (****$P < 0.0001$, ***$P < 0.001$, **$P < 0.01$, *$P < 0.05$). Fold change calculated via $2^{(-ddCT)}$ method. cap = caput. Sham 10 days, testis $n = 6$, caput $n = 4$; UPEC 10 days, testis $n = 5$, caput $n = 4$.

corpus and cauda epididymidis displayed a very similar gene expression pattern, which was visibly different from the respective patterns of caput epididymidis and testis (Fig. 4A). In this regard, immune-related genes were amongst the most prominent differentially-regulated genes (Fig. 4B). Further analysing a more specific gene set 'defense response to bacterium' (GO: 0042742, Fig. 4C), high baseline levels of

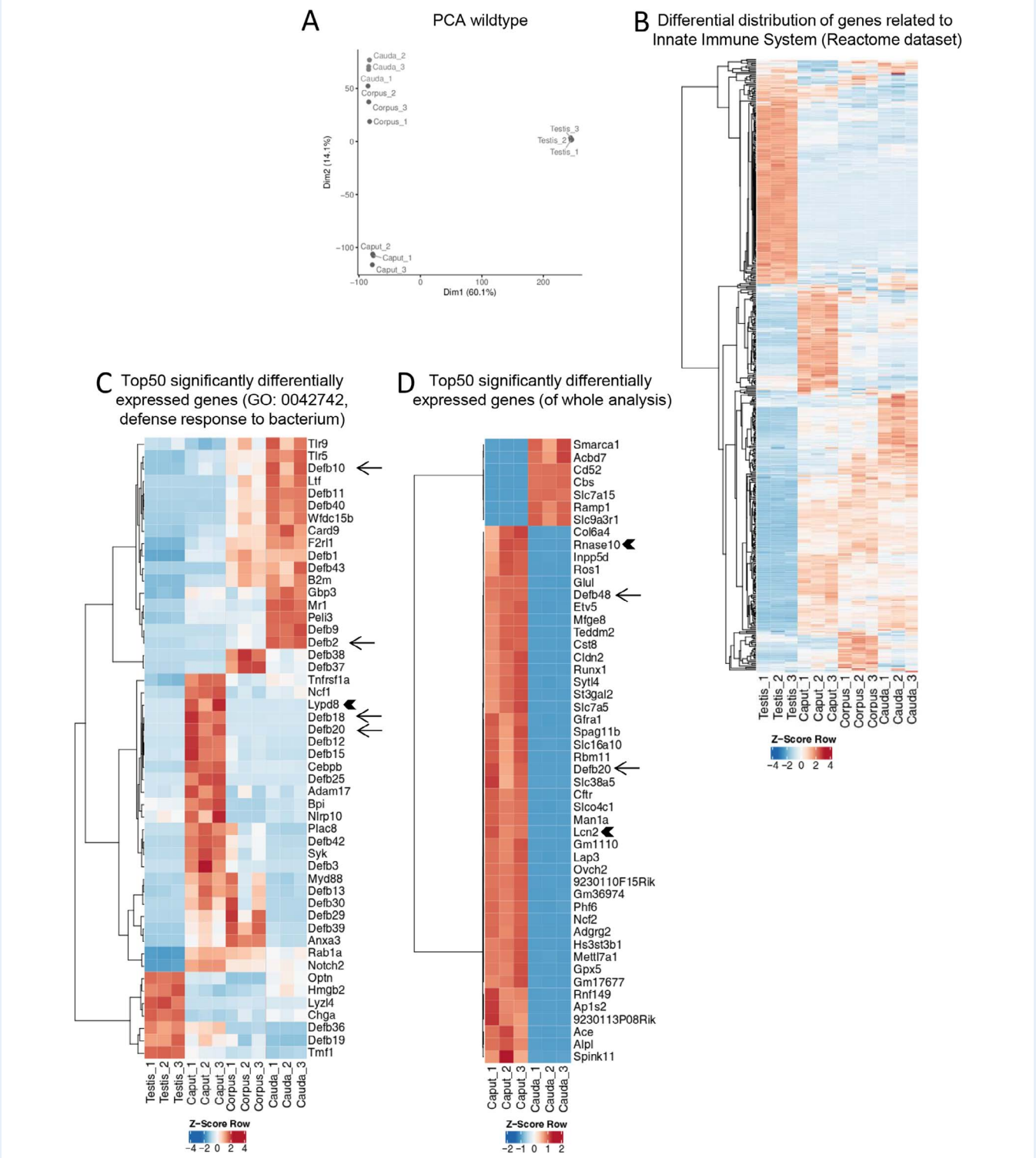


**Figure 4 Whole transcriptome analysis of testis, and caput, corpus and cauda epididymidis of wild-type mice.** (**A**) Principal component analysis (PCA) presenting differences in global gene signatures associated with the different tissues. (**B**) Heat map showing significantly differentially expressed genes within term 'Innate Immune System' from Reactome database in caput, cauda and corpus epididymidis and testis (based on false discovery rate (FDR) > 0.05 and minimal count number > 20, presented with *Z*-score normalisation). (**C**) Heat map of top 50 differentially expressed genes of a published dataset (GO: 0042742, 'defense response to bacterium') in caput, cauda and corpus epididymidis and testis (based on FDR > 0.05, base mean > 20, presented with *Z*-score normalisation). (**D**) Heat map of top 50 significantly differentially expressed genes of the whole dataset between caput and cauda epididymidis (based on FDR > 0.05, base mean > 20, presented with Z-score normalisation). Arrows pointing at selected beta-defensins, arrow heads pointing at other antimicrobial peptides of interest.

antimicrobial factors (arrowhead), including many beta-defensins (exemplary black arrows), were detected in both caput and cauda epididymidis (Fig. 4C, Supplementary Table SII). Interestingly, expression of certain beta-defensins was spatially very different (e.g. significantly higher expression of *Defb10*, *Defb2* in the cauda; significantly higher expression of *Defb18*, *Defb20* in the caput; Fig. 4C, Supplementary Table SII). Antimicrobial factors were also found amongst the top 50 most differentially expressed genes between caput and cauda epididymidis with *Rnase10* and *Lcn2* (Lipocalin 2; protective role in UPEC infection of the bladder; Terlizzi *et al.*, 2017; Schwartz *et al.*, 2018) significantly higher in the caput epididymidis (Fig. 4D). Reliability of the RNA-seq data was validated by RT-qPCR expression analysis of selected markers using different samples of normal wild-type testis, caput and cauda epididymidis (Supplementary Fig. S3). Validation showed that mRNA expression data generated by RT-qPCR (graphs) matched the RNA-seq data expressed as library-sized normalised counts (graphs and table in Supplementary Fig. S3).

## Effect of UPEC infection on expression of beta-defensins and UPEC-associated antimicrobial factors in caput and cauda epididymidis *in vivo*. Influence of LYPD8 on bacterial epithelial adherence *in vitro*

Beta-defensins with different spatial expression patterns in normal wild-type caput and cauda epididymidis were selected for further examination in infected tissues (Fig. 5, Supplementary Fig. S3). In control mice, expression levels of *Defb20* and *Defb21* mRNA were enhanced in the caput (Supplementary Fig. S3). Following infection, a significant decrease in *Defb20* was seen in both caput and cauda epididymidis, whilst Defb21 remained unchanged. Following infection, both *Defb2* and *Defb28* showed a significant downregulation from high mRNA levels in the cauda epididymidis, along with a tendency towards increased expression levels observed in the caput epididymidis (Fig. 5A). In contrast, other host antimicrobial factors with known involvement in UPEC infections showed an overall increase upon infection (Fig. 5B). In this regard, *Lcn2* (siderophore-binding protein) and *Ptx3* (Pentraxin3, soluble pattern recognition receptor) mRNA were significantly upregulated in the cauda epididymidis following infection. In contrast, for *Camp* (Cathelicidin) and *Lypd8* (Ly6/PLAUR domain containing 8 protein) an increased trend of mRNA expression was noted in both caput and cauda epididymidis following infection (Fig. 5B).

Because this is the first report of *Lypd8* mRNA expression in the rodent epididymis, the synthesis and possible functions of this molecule were further examined. Using laser microdissection, expression of *Lypd8* mRNA was found in dissected caput epididymidis epithelial cells, but not in the respective interstitial compartment (Fig. 5C). Application of an *in vitro* assay in which MEPC5 cells (mouse caput epididymal epithelial cell line) were co-cultured with UPEC CFT073 in the presence or absence of human recombinant LYPD8 indicated an LYPD8-associated reduction of bacterial adherence to these cells (Fig. 5D).

# Discussion

Bacterial AEO results in sub- or infertility in ~40% of patients. The underlying reasons are diverse and can involve obstructive azoospermia, persistent epididymal induration needing surgical intervention or testicular aetiologies such as oligozoospermia (Schuppe *et al.*, 2017). Consistent with clinical data, further information from rodent studies of bacterial AEO show that tissue scarring and fibrotic changes that mainly develop in the cauda epididymidis were largely irreversible and remained resistant to standard antibiotic therapy (Ludwig *et al.*, 2002; Michel *et al.*, 2016; Michel *et al.*, 2015; Stammler *et al.*, 2015; Klein *et al.*, 2019). Whilst the pathological consequences of AEO for the epididymal tissues are fairly consistently reported in the literature for both men and rodent models, long-term consequences of bacterial AEO for the testis are less clear (Demir *et al.*, 2007; Pilatz *et al.*, 2015; Rana & Prabha, 2018). Notably, the respective animal studies vary profoundly with regards to the infectious doses of *E. coli* ($10^4$ to $10^8$ CFU per infections) as well as the type or the therapeutic doses of antibiotics applied. Similar differences play a role in orchitis and/or epididymitis studies in which LPS as an isolated UPEC virulence factor is used for induction. For those, likewise, a correlation between the applied dose of LPS and the potential long-term impairment of spermatogenesis was suggested (Wang *et al.*, 2019). In at least one study in men, normalisation of testicular parameters has been reported in 80% of AEO patients 3 months after therapeutic intervention (Pilatz *et al.*, 2013). In the present bacterial AEO mouse model, immunofluorescence analysis revealed that F4/80-positive cells, i.e. mononuclear phagocytes as the main type of testis-infiltrating immune cells detectable during AEO, were increased in the testicular interstitium at Day 10 p.i. Notably, no other immune cell types were analysed in this study. Coincidentally, inside the seminiferous tubules, spermatogenic disruption affecting mostly haploid germ cells, particularly elongating spermatids, was only visible at Day 10 p.i. Staining with PCNA further indicated that, in spite of the presence of bacteria at Day 10 p.i., the testes did not completely lose their proliferative spermatogenic potential (at Day 10 p.i., PCNA-positive nuclei were still detectable in ~60% of tubule cross-sections). Together with the observed small increase in classical pro-inflammatory testicular cytokine expression, it appears likely that in the AEO model utilised, the spermatogenic impairment observed at Day 10 p.i. was less likely derived from the organ's inflammatory response towards the pathogen, but rather from the presence of UPEC virulence factors, such as sperm agglutination factor, sperm immobilisation factor, cytotoxic necrotising factor, alpha-haemolysin or LPS, which have all been established to negatively impact viability or function of spermatozoa (Diemer *et al.*, 2003; Schulz *et al.*, 2010; Cools, 2017; Villegas *et al.*, 2017). Notably, the negative effects on spermatozoa are higher with haemolytic *E. coli* strains that are also known to induce more severe epididymitis (Lang *et al.*, 2013; Villegas *et al.*, 2017). Support for a direct effect of luminal bacteria on germ cells is also based on a previous study by Nagaosa *et al.*, which reported that only intratubular, but not interstitial, injection of live *E. coli* resulted in spermatogenic damage (Nagaosa *et al.*, 2009). In our bacterial AEO model, the antimicrobial therapy using levofloxacin could not protect the cauda epididymidis from long-term fibrosis and ductal obstruction (Klein *et al.*, 2019), whereas on the testicular level partially rescue/protection from spermatogenic damage was achieved with levofloxacin treatment (data not shown), but surprisingly also without any intervention. Altogether, these data support the concept that the initial spermatogenic impairment associated with UPEC-induced AEO is largely due to a direct bacterial effect on spermatozoa, whereas the testis can maintain its capacity for

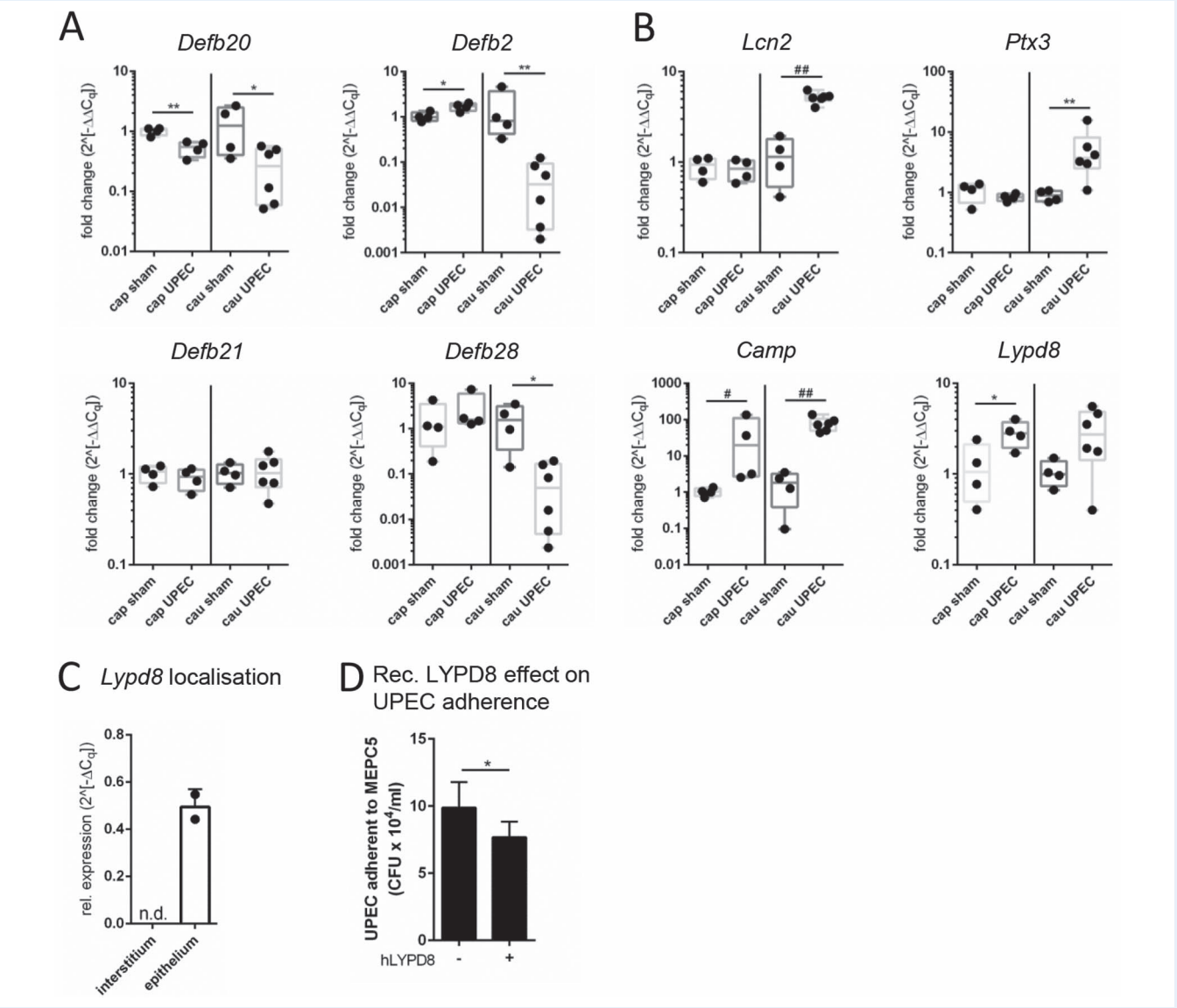


**Figure 5 RT-qPCR analysis and comparison of modulation of antimicrobial factors in caput and cauda epididymidis and Lypd8 assessment in mouse and *in vitro* assay.** (**A**) beta-defensins, (**B**) UPEC-associated antimicrobial factors. Unpaired *t* test (*) or Mann–Whitney *U* test (#) for each organ, respectively, comparing sham to UPEC-infected mice (****$P < 0.0001$, ***$P < 0.001$, **$P < 0.01$, *$P < 0.05$). Fold change calculated via $2^{(-ddCT)}$ method. Data presented as box-and-whisker with median and min/max. cap = caput, cau = cauda. Sham 10 days, caput $n = 4$, cauda $n = 4$; UPEC 10 days, caput $n = 4$, cauda $n = 6$. (**C**) Laser-assisted microdissection of caput epithelium and caput interstitium from wild-type epididymis, $n = 2$. Relative expression calculated via $2^{(-dCT)}$ method. Data presented as mean ± SD. (**D**) Bacterial adherence to MEPC5 cells under the presence (+) or absence (−) of 1 µg/ml human recombinant LYPD8 (hLYPD8). CFU/ml were calculated after incubation of agar plates at 37°C for 24 h. Summary of three independent experiments with each time $n = 2$–3 per group. Unpaired *t* test comparing the number of MEPC5-adherent UPEC in the presence or absence of LYPD8 (****$P < 0.0001$, ***$P < 0.001$, **$P < 0.01$, *$P < 0.05$).

spermatogenesis. In summation, rodent as well as clinical data suggest that epididymal obstruction in the cauda epididymidis rather than testicular impairment may be responsible for long-term detrimental effects on fertility following AEO (Pilatz *et al*., 2013; Schuppe *et al*., 2017).

Although the epididymis consists of one single highly convoluted duct embedded in an interstitial tissue, it is acknowledged that the different epididymal regions or segments differ fundamentally, with each segment showing a different region-specific cellular composition and expressing a characteristic set of genes (Turner *et al*., 2003; Hsia & Cornwall, 2004; Johnston *et al*., 2005; Jelinsky *et al*., 2007; Domeniconi *et al*., 2016; Battistone *et al*., 2019a, 2019b). In relation to the immune status, Browne *et al*. investigated the different epididymal regions of the human epididymis and identified a distinct immunosuppressive phenotype specific to the caput epididymidis. In contrast, corpus and cauda epididymidis were shown to be immunologically similar, but distinct from the caput with high expression of genes associated with innate immunity and immune defense

(Browne *et al*., 2016). As mentioned earlier, RNA-sequencing of total RNA isolated from different epididymal regions will expectedly present very distinct mRNA profiles. This approach and technique hence allow us to collect holistic information about the 'transcriptional environment' of different organs, the epididymal regions and the testis, respectively, to better understand their unique inherent immune environments. In line with that, Browne's observation from the human matches the whole transcriptome analysis from mouse performed in the present study, in which also a profoundly different repertoire of immune-related genes was found enriched in the cauda as opposed to the caput epididymidis, with the corpus showing a profile closer to the cauda region. Of note, some immunological key factors important for the establishment of UPEC infections, such as uroplakin1b (*Upk1b*, essential for UPEC adherence to epithelia, Thumbikat *et al*., 2009), Toll-like-receptor 4 (*Tlr4*, archetypical Tlr for recognition of bacteria; Hilbert, 2011) or *Myd88* (adaptor protein fundamentally involved in induction of immune responses; Deguine & Barton (2014) were highly expressed in the caput epididymidis, based on our RNA-seq analysis. Thus, a global immunological suppression cannot conclusively serve as an explanation for the preservation of normal organ integrity observed for the caput epididymidis in our bacterial AEO model. Similar to the study conducted by Silva *et al*. on the cauda epididymidis (Silva *et al*., 2018), analyses of the early phase of infection are now required to clarify the possibility that an acute pro-inflammatory response in the caput epididymidis may be elicited early and resolved already before Day 10 p.i. Another protective mechanism established in the proximal regions of the epididymis could rely on a particularly effective host defence by, for example, (i) higher proportions of intraepithelial lumen-sampling immune cells (Voisin *et al*., 2018; Battistone *et al*., 2019b) or (ii) the high expression of a large number of antimicrobial peptides such as beta-defensins, which has been reported by several studies including this one (Com *et al*., 2003; Ribeiro *et al*., 2012; Battistone *et al*., 2019a ). Whereas our RNA-seq data revealed high baseline expression levels of different beta-defensins in the caput and cauda region, under infectious conditions mRNA levels of selected beta-defensins were at best slightly upregulated or significantly downregulated. As a limitation, protein expression levels complementing the qPCR results were not assessed in the present study. Also, beta-defensins are established to be mainly expressed by epithelial cells, recently specified as epithelial clear cells, in the epididymis (Battistone *et al*., 2019a). Hence, the reduction of beta-defensin transcripts in infected caudae epididymides needs to be interpreted with caution as it may be caused by a relative loss or displacement of epithelial cells in the cauda concomitant to a superimposing effect of leucocytic infiltration.

As additional mechanisms may be in place that act in concert with the beta-defensins to confer protection, we also investigated other antimicrobial factors with well-known functions in control and clearance of UPEC-elicited urinary tract infections (Zasloff, 2007; Okumura *et al*., 2016; Terlizzi *et al*., 2017). In this regard, expression of lipocalin 2 (*Lcn2*), cathelicidin (*Camp*), pentraxin 3 (*Ptx3*) and *Lypd8* were all found to be substantially increased in the cauda and, to a lesser extent, in the caput epididymidis following infection. Importantly, in contrast to beta-defensins, some of these antimicrobial peptides can be produced by both epithelial as well as immune cells. In more detail, pentraxin 3 as a soluble pattern recognition receptor can promote bacterial uptake by neutrophils (Kunes *et al*., 2012; Jaillon *et al*., 2014; Terlizzi *et al*., 2017). Hence, higher expression levels of pentraxin 3 in the cauda epididymidis can be readily associated with the massive invasion of neutrophils detectable in this region following bacterial AEO (Klein *et al*., 2019; Kunes *et al*., 2012). Cathelicidin, known to be rapidly induced upon pathogen recognition, can in turn prompt local production of antimicrobial peptides, bacterial lysis and LPS-neutralisation (Wertenbruch *et al*., 2015; Terlizzi *et al*., 2017). Of note, as shown in our transcriptomic analysis, lipocalin 2 belongs to the top 50 significantly differentially expressed genes in the caput versus cauda epididymidis with a very high basal expression level in the caput region. This protein binds to bacterial siderophores, thereby inducing an iron deprivation that subsequently fundamentally limits bacterial growth and enhances phagocytic bacterial clearance (Toyonaga *et al*., 2016; Terlizzi *et al*., 2017). Hence, along with other antimicrobial peptides, lipocalin 2 may play a crucial role in establishing efficient protection from invading bacteria in the caput region.

*Lypd8* also belongs to the top 50 differentially expressed genes in caput versus cauda epididymidis with high expression levels confined to the caput. Recently, a specific effect for *Lypd8* in controlling gram-negative bacterial infections has been reported for the gut. In that report, Okumura *et al*. identified the capability of LYPD8 to bind polymerised flagellin, which is found in bacterial flagella/fimbriae/pili, thereby preventing bacterial adherence from bacteria such as *E. coli* to the epithelium of the colon. The LYPD8-induced segregation of intestinal bacteria from the epithelial surface is thought to be one mechanism maintaining the intestinal homeostasis in view of a large number of microbes constantly being present in this organ (Okumura *et al*., 2016). As discovered from UPEC infection of the bladder, initial adherence of UPEC to the epithelial surface is essential for subsequent internalisation, host colonisation and induction of cytokine expression (Ribet & Cossart, 2015; Lewis *et al*., 2016). In contrast to the cauda epididymidis, in which a strong, long-lasting induction of pro-inflammatory cytokine production correlates with a massive immune cell infiltration, UPEC challenge of the caput epididymidis did not result in higher pro-inflammatory cytokine levels or any evident morphological alteration detectable at Day 10 p.i., whereas some AMP transcript levels were altered. It cannot be excluded though that stronger immune responses or tissue alterations occur and resolve before Day 10 p.i. This point would warrant attention in a complementary study, possibly combined with experiments that discriminate whether (i) the caput is less capable of mounting pro-inflammatory responses to UPEC or whether (ii) in the caput, bacteria are more effectively controlled by a large spectrum of inherently expressed anti-microbial factors. In this scenario, LYPD8 as an *E. coli* fimbriae-binding factor, which is uniquely and at high levels expressed in the caput epididymidis, may locally affect bacterial epithelial adherence and impact UPEC before it becomes destructive. Using an *in vitro* adherence assay, our data suggest that LYPD8 protein is indeed able to reduce the adherence of UPEC to a caput epididymal epithelial cell line supporting this notion.

Taken together, several abundant antimicrobial factors, including beta-defensins and other antimicrobial peptides, such as lipocalin 2 and LYPD8, which function in the restriction of bacterial nutrients and inhibition of bacterial adherence to host cells, respectively, may act together to render the caput luminal environment less hospitable for pathogens, thereby safe-guarding it from bacterial induced tissue damage.

## Supplementary data

Supplementary data are available at *Molecular Human Reproduction* online.

## Acknowledgements

The scientific expertise and help of Michael Rothballer, Juri Schklarenko, Martina Hudel and Julia Baldauf throughout the study are highly acknowledged.

## Authors' roles

B.K. carried out experiments and analysed data. S.G. performed WTA analysis and preparation of respective figures. S.B. carried out infection experiments. B.K., M.P.H., K.L.L., R.M. and A.M. were responsible for study design. B.K., S.B., A.M., M.P.H., K.L.L., R.M. and A.M. were involved in writing and critical revision of manuscript. All authors gave final approval of the submitted and published version.

## Funding

Deutsche Forschungsgemeinschaft (DFG), Monash University, and the Medical Faculty of Justus-Liebig University to the International Research Training Group on 'Molecular pathogenesis of male reproductive disorders' (GRK 1871); National Health and Medical Research Council of Australia (ID1079646, ID1081987, ID1020269 and ID1063843 to K.L.L. and M.P.H.); Victorian Government's Operational Infrastructure Support Program.

## Conflict of interest

None declared.

## References

Andrews S. 2010**.** *FastQC: A Quality Control Tool for High Throughput Sequence Data*. Available online at: http://www.bioinformatics.babraham.ac.uk/projects/fastqc.

Banyra O, Shulyak A. Acute epididymo-orchitis: staging and treatment. *Cent European J Urol* 2012;**65**:139–143.

Battistone MA, Spallanzani RG, Mendelsohn AC, Capen D, Nair AV, Brown D, Breton S. Novel role of proton-secreting epithelial cells in sperm maturation and mucosal immunity. *J Cell Sci* 2019a;**133**.

Battistone MA, Mendelsohn AC, German SR, Dennis B, Nair AV, Breton S. Region-specific transcriptomic and functional signatures of mononuclear phagocytes in the epididymis. *Mol Hum Reprod* 2019b; gaz059.

Bhushan S, Hossain H, Lu Y, Geisler A, Tchatalbachev S, Mikulski Z, Schuler G, Klug J, Pilatz A, Wagenlehner F *et al*. Uropathogenic E. coli induce different immune response in testicular and peritoneal macrophages: implications for testicular immune privilege. *PLoS One* 2011;**6**:1–15.

Biswas B, Bhushan S, Rajesh A, Suraj SK, Lu Y, Meinhardt A, Yenugu S. Uropathogenic Escherichia coli (UPEC) induced antimicrobial gene expression in the male reproductive tract of rat: evaluation of the potential of defensin 21 to limit infection. *Andrology* 2015;**3**:368–375.

Bolger AM, Lohse M, Usadel B. Trimmomatic: a flexible trimmer for Illumina sequence data. *Bioinformatics* 2014;**30**:2114–2120.

Browne JA, Yang R, Leir S, Eggener SE, Harris A. Expression profiles of human epididymis epithelial cells reveal the functional diversity of caput, corpus and cauda regions. *Mol Hum Reprod* 2016;**22**:69–82.

Cao D, Li Y, Yang R, Wang Y, Zhou Y, Diao H, Zhao Y, Zhang Y, Lu J. Lipopolysaccharide-induced epididymitis disrupts epididymal beta-defensin expression and inhibits sperm motility in rats. *Biol Reprod* 2010;**83**:1064–1070.

Com E, Bourgeon F, Evrard B, Ganz T, Colleu D, Jégou B, Pineau C. Expression of antimicrobial defensins in the male reproductive tract of rats, mice, and humans. *Biol Reprod* 2003;**68**:95–104.

Cools P. The role of Escherichia coli in reproductive health: state of the art. *Res Microbiol* 2017;**168**:892–901.

Deguine J, Barton GM. MyD88: a central player in innate immune signaling. *F1000Prime Rep* 2014;**6**:1–7.

Demir A, Türker P, Önol FF, Sirvanci S, Findik A, Tarcan T. Effect of experimentally induced Escherichia coli epididymo-orchitis and ciprofloxacin treatment on rat spermatogenesis. *Int J Urol* 2007;**14**:268–272.

Diemer T, Huwe P, Ludwig M, Hauck EW, Weidner W. Urogenital infection and sperm motility. *Andrologia* 2003;**35**:283–287.

Dobin A, Davis CA, Schlesinger F, Drenkow J, Zaleski C, Jha S, Batut P, Chaisson M, Gingeras TR. STAR: ultrafast universal RNA-seq aligner. *Bioinformatics* 2013;**29**:15–21.

Domeniconi RF, Souza AC, Xu B, Washington AM, Hinton BT. Is the epididymis a series of organs placed side by side? *Biol Reprod* 2016;**95**:1–8.

Fei Z, Hu S, Xiao L, Zhou J, Diao H, Yu H, Fang S, Wang Y, Wan Y, Wang W *et al*. mBin1b transgenic mice show enhanced resistance to epididymal infection by bacteria challenge. *Genes Immun* 2012;**13**:445–451.

Fijak M, Pilatz A, Hedger MP, Nicolas N, Bhushan S, Michel V, Tung KSK, Schuppe HC, Meinhardt A. Infectious, inflammatory and "autoimmune" male factor infertility: how do rodent models inform clinical practice? *Hum Reprod Update* 2018;**24**:416–441.

Hilbert DW. Uropathogenic Escherichia Coli: The pre-eminent urinary tract infection pathogen. In: *E. coli Infections: Causes, Treatment and Prevention*. New York: Nova Science Publishers, 2011.

Hsia N, Cornwall GA. DNA microarray analysis of region-specific gene Expressio in the mouse epididymis. *Biol Reprod* 2004;**70**:448–457.

Jaillon S, Moalli F, Ragnarsdottir B, Bonavita E, Puthia M, Riva F, Barbati E, Nebuloni M, Krajinovic LC, Markotic A *et al*. The humoral pattern recognition molecule PTX3 is a key component of innate immunity against urinary tract infection. *Immunity* 2014;**40**:621–632.

Jelinsky SA, Turner TT, Bang HJ, Finger JN, Solarz MK, Wilson E, Brown EL, Kopf GS, Johnston DS. The rat epididymal transcriptome: comparison of segmental gene expression in the rat and mouse epididymides. *Biol Reprod* 2007;**76**:561–570.

Johnsen SG. Testicular biopsy score count - a method for registration of spermatogenesis in human testes: normal values and results in 335 hypogonadal males. *Hormones* 1970;**1**:2–25.

Johnston DS, Jelinsky SA, Bang HJ, DiCandeloro P, Wilson E, Kopf GS, Turner TT. The mouse epididymal transcriptome: transcriptional

profiling of segmental gene expression in the epididymis. *Biol Reprod* 2005;**73**:404–413.

Klein B, Pant S, Bhushan S, Kautz J, Rudat C, Kispert A, Pilatz A, Wijayarathna R, Middendorff R, Loveland KL *et al.* Dexamethasone improves therapeutic outcomes in a preclinical bacterial epididymitis mouse model. *Hum Reprod* 2019;dez073:1–11.

Kunes P, Holubcova Z, Kolackova M, Krejsek J. Pentraxin 3 ( PTX 3 ): an endogenous modulator of the inflammatory response. *Mediators Inflamm* 2012;920517.

Lang T, Dechant M, Sanchez V, Wistuba J, Boiani M, Pilatz A, Stammler A, Middendorff R, Schuler G, Bhushan S *et al.* Structural and functional integrity of spermatozoa is compromised as a consequence of acute uropathogenic *E. coli*-associated epididymitis. *Biol Reprod* 2013;**89**:1–10.

Letourneau J, Levesque C, Berthiaume F, Jacques M, Mourez M. In vitro assay of bacterial adhesion onto mammalian epithelial cells. *J Vis Exp* 2011;**16**:3–6.

Lewis AJ, Richards AC, Mulvey MA. Invasion of host cells and tissues by uropathogenic bacteria. *Microbiol Spectr* 2016;**4**:1–29.

Liao Y, Smyth GK, Shi W. featureCounts: an efficient general purpose program for assigning sequence reads to genomic features. *Bioinformatics* 2013;**30**:923–930.

Love MI, Huber W, Anders S. Moderated estimation of fold change and dispersion for RNA-seq data with DESeq2. *Genome Biol* 2014; **15**:1–21.

Lu Y, Bhushan S, Tchatalbachev S, Marconi M, Bergmann M, Weidner W, Chakraborty T, Meinhardt A. Necrosis is the dominant cell death pathway in uropathogenic *Escherichia coli* elicited epididymo-orchitis and is responsible for damage of rat testis. *PLoS ONE* 2013;**8**:1–15.

Ludwig M, Johannes S, Bergmann M, Failing K, Schiefer HG, Weidner W. Experimental Escherichia coli epididymitis in rats : a model to assess the outcome of antibiotic treatment. *BJU Int* 2002;**90**:933–938.

Michel V, Duan Y, Stoschek E, Bhushan S, Middendorff R, Young JM, Loveland KL, DeKretser DM, Hedger MP, Meinhardt A. Uropathogenic Escherichia coli causes fibrotic remodelling of the epididymis. *J Pathol* 2016;**240**:15–24.

Michel V, Pilatz A, Hedger MP, Meinhardt A. Epididymitis: revelations at the convergence of clinical and basic sciences. *Asian J Androl* 2015; **17**:756–763.

Nagaosa K, Nakashima C, Kishimoto A, Nakanishi Y. Immune response to bacteria in seminiferous epithelium. *Reproduction* 2009;**137**: 879–888.

Okumura R, Kurakawa T, Nakano T, Kayama H, Kinoshita M, Motooka D, Goto K, Kimura T, Kamiyama N, Kusu T *et al.* Lypd8 promotes the segregation of flagellated microbiota and colonic epithelia. *Nature* 2016;**532**:117–121.

Pilatz A, Boecker M, Schuppe HC, Wagenleher F. Current aspects of epididymo-orchitis. *Aktuel Urol* 2016;**47**:237–242.

Pilatz A, Wagenlehner F, Bschleipfer T, Schuppe HC, Diemer T, Linn T, Weider W, Altinkilic B. Acute epididymitis in ultrasound: results of a prospective study with baseline and follow-up investigations in 134 patients. *Euro J Radiol* 2013;**82**:e762–e768.

Pilatz A, Ceylan I, Schuppe HC, Ludwig M, Fijak M, Chakraborty T, Weidner W, Bergmann M, Wagenlehner F. Experimental *Escherichia coli* epididymitis in rats: assessment of testicular involvement in a long-term follow-up. *Andrologia* 2015;**47**:160–167.

Rana K, Prabha V. Sperm agglutinating *Escherichia coli* and male infertility: an *in vivo* study. *Ann Infert Rep Endocrin* 2018;**1**:1–7.

Ribeiro CM, Romano RM, Avellar MCW. Beta-defensins in the epididymis: clues to multifunctional roles. *Anim Reprod* 2012;**9**:751–759.

Ribet D, Cossart P. How bacterial pathogens colonize their hosts and invade deeper tissues. *Microbes Infect* 2015;**17**:173–183.

Rusz A, Pilatz A, Wagenlehner F, Linn T, Diemer T, Schuppe HC, Lohmeyer J, Hossain H, Weidner W. Influence of urogenital infections and inflammation on semen quality and male fertility. *World J Urol* 2012;**30**:23–30.

Schuppe HC, Pilatz A, Hossain H, Meinhardt A, Bergmann M, Haidl G, Weidner W. Orchitis und Infertilität. *Urologe* 2010;**49**:629–635.

Schuppe HC, Meinhardt A, Allam JP, Bergmann M, Weidner W, Haidl G. Chronic orchitis: a neglected cause of male infertility? *Andrologia* 2008;**40**:84–91.

Schuppe HC, Pilatz A, Hossain H, Diemer T, Wagenlehner F, Weidner W. Urogenital infection as a risk factor for male infertility. *Dtsch Arztebl Int* 2017;**114**:339–346.

Schulz M, Sánchez R, Soto L, Risopatrón J, Villegas J. Effect of *Escherichia coli* and its soluble factors on mitochondrial membrane potential, phosphatidylserine translocation, viability, and motility of human spermatozoa. *Fertil Steril* 2010;**94**:619–623.

Schwartz L, Cohen A, Thomas J, Spencer JD. The immunomodulatory and antimicrobial properties of the vertebrate ribonuclease a superfamily. *Vaccine* 2018;**6**:1–19.

Silva EJR, Ribeiro CM, Miriam AFM, Silva AAS, Romano RM, Hallak J, Avellar MCW. Lipopolysaccharide and lipotheicoic acid differentially modulate epididymal cytokine and chemokine profiles and sperm parameters in experimental acute epididymitis. *Sci Rep* 2018;**8**:103.

Stammler A, Hau T, Bhushan S, Meinhardt A, Jonigk D, Lippmann T, Pilatz A, Schneider-Hüther I, Middendorff R. Epididymitis: ascending infection restricted by segmental boundaries. *Hum Reprod* 2015;**30**:1557–1565.

Street EJ, Justice ED, Kopa Z, Portman MD, Ross JD, Skerlev M, Wilson JD, Patel R. The 2016 European guideline on the management of epididymo-orchitis. *Int J STD AIDS* 2017;**28**:744–749.

Tabuchi Y, Toyama Y, Toshimori K, Komiyama M, Mori C, Kondo T. Functional characterization of a conditionally immortalized mouse epididymis caput epithelial cell line MEPC5 using temperature-sensitive simian virus 40 large T-antigen. *Biochem Biophys Res Commun* 2005;**329**:812–823.

Terlizzi ME, Gribaudo G, Maffei ME. UroPathogenic *Escherichia coli* (UPEC) infections: virulence factors, bladder responses, antibiotic, and non-antibiotic antimicrobial strategies. *Front Microbiol* 2017; **8**:1–23.

Thumbikat P, Berry RE, Zhou G, Billips BK, Yaggie RE, Zaichuk T, Sun TT, Schaeffer AJ, Klumpp DJ. Bacteria-induced uroplakin signaling mediates bladder response to infection. *PLoS Pathog* 2009;**5**:1–17.

Toyonaga T, Matsuura M, Mori K, Honzawa Y, Minami N, Yamada S, Kobayashi T, Hibi T, Nakase H. Lipocalin 2 prevents intestinal inflammation by enhancing phagocytic bacterial clearance in macrophages. *Sci Rep* 2016;**6**:1–13.

Turner TT, Bomgardner D, Jacobs JP, Nguyen QAT. Association of segmentation of the epididymal interstitium with segmented tubule function in rats and mice. *Reproduction* 2003;**125**:871–878.

UniProt Consortium. Activities at the universal protein resource (UniProt). *Nucleic Acids Res* 2014;**42**:191–198.

Villegas JV, Boguen R, Uribe P. Effect of Uropathogenic *Escherichia coli* on Human Sperm Function and Male Fertility. In: *Escherichia coli - Recent Advances on Physiology, Pathogenesis and Biotechnological Applications*. London: InTech Open, 2017.

Voisin A, Whitfield M, Damon-Soubeyrand C, Goubely C, Henry-Berger J, Saez F, Kocer A, Drevet JR, Guiton R. Comprehensive overview of murine epididymal mononuclear phagocytes and lymphocytes: unexpected populations arise. *J Reprod Immunol* 2018;**126**:11–17.

Wang F, Liu W, Jiang Q, Gong M, Chen R, Wu H, Han R, Chen Y, Han D. Lipopolysaccharide-induced testicular dysfunction and epididymitis in mice: a critical role of tumor necrosis factor alpha. *Biol Reprod* 2019;**100**:849–861.

Welch RA. Uropathogenic *Escherichia coli*-associated exotoxins. *Microbiol Spectr* 2016;**4**:1–16.

Wertenbruch S, Drescher H, Grossarth V, Kroy DC, Giebeler A, Erschfeld S, Heinrichs D, Soehnlein O, Trautwein C, Brandenburg LO *et al.* The antimicrobial peptide LL-37 / CRAMP is elevated in patients with liver diseases and acts as a protective factor during mouse liver injury. *Digestion* 2015;**91**:307–317.

Zasloff M. Antimicrobial peptides, innate immunity, and the normally sterile urinary tract. *JASN* 2007;**18**:2810–2816.